Arabian Journal of Chemistry (2023) **16**, 104852

King Saud University

Arabian Journal of Chemistry

www.ksu.edu.sa
www.sciencedirect.com

ORIGINAL ARTICLE

Design, synthesis and biological activity of chalcone derivatives containing pyridazine

Shuai Chen [a], Miaohe Zhang [a], Shuang Feng [a], Chenyu Gong [a], Yuanxiang Zhou [a], Li Xing [a], Bangcan He [a], Yongjun Wu [b,*], Wei Xue [a,*]

[a] *State Key Laboratory Breeding Base of Green Pesticide and Agricultural Bioengineering, Key Laboratory of Green Pesticide and Agricultural Bioengineering, Ministry of Education, Research and Development Center for Fine Chemicals, Guizhou University, Guiyang 550025, PR China*
[b] *Key Laboratory of Plant Resource Conservation and Germplasm Innovation in Mountainous Region (Ministry of Education), College of Life Sciences, Guizhou University, Guiyang 550025, Guizhou Province, China*

Received 6 November 2022; accepted 21 March 2023
Available online 27 March 2023

KEYWORDS

Chalcone derivatives;
Pyridazine;
Antifungal activity;
Antibacterial activity;
Mechanism of action

Abstract Inspired by the application of fungicide from natural products, a series of chalcone derivatives containing pyridazine were designed, synthesized, and evaluated for their antifungal activities against nine plant fungi and antibacterial activity against three plant bacteria. The antibacterial results revealed that **B8** showed the best activity against *Xanthomonas campestris pv. citri* (*Xac*) with an EC_{50} value of 78.89 μg/mL, superior to Bismerthiazol (EC_{50} = 86.72 μg/mL). The antifungal bioactivity results showed that some of the compounds had good bioactivity against fungi, such as **B4** showed the best bioactivity against *Botrytis cinerea* (*BC*) with an EC_{50} value of 8.91 μg/mL, which was better than the azoxystrobin (EC_{50} = 20.28 μg/mL). Compounds **B4**, **D2** and **D3** showed good biological activity against *Rhizoctonia solani* (*RS*), with an EC_{50} value of 18.10, 20.18 and 20.60 μg/mL, comparable to the azoxystrobin. Antifungal mechanism studies of *BC* by **B4** suggest that **B4** disrupts the cell membrane of the mycelium and thus inhibits the growth of the fungus. The above indicates that chalcone derivatives containing pyridazine have the potential to become fungicides.

1. Introduction

Plant-pathogenic fungi cause huge economic losses in global agricultural production every year and seriously threaten to human health and food safety (Silva et al., 2019). *Botrytis cinerea*, the causal agent of gray mold in plants, has a wide host range and is one of the most damaging diseases in the world currently (Dean et al., 2012). It can infect plants' roots, leaves, flowers, and fruits, causing yield reduction in many crops and fruit rot (Williamson et al., 2007, Li et al., 2018). In addition, *Xoo*, *Xac*, and *Psa* can cause yield reduction of major

* Corresponding authors.
E-mail addresses: wyjbio@163.com (Y. Wu), wxue@gzu.edu.cn (W. Xue).

Peer review under responsibility of King Saud University.

Production and hosting by Elsevier

https://doi.org/10.1016/j.arabjc.2023.104852
1878-5352

crops every year (Shasmita et al., 2019, Wu et al., 2021). Currently, plant pathogenic fungi and bacteria are still mainly controlled by means of chemical fungicides, which are not only easy to cause environmental pollution (Muller et al., 2019, Zubrod et al., 2019), but also prone to resistance (Lu et al., 2014, Ma et al., 2018), so there is a need to continuously develop new high-efficiency, low-toxicity fungicides.

Chalcone is precursor for the biosynthesis of natural product flavonoids. Chalcone is part of the plants most prominent class of secondary metabolites. (Tomar et al., 2009, Funakoshi-Tago et al., 2015). Chalcone and its derivatives are widely used in fungicides because of their good anti-fungal (Zhou et al., 2022), anti-bacterial (Dkhar et al., 2020), anti-viral (Gan et al., 2017), insecticidal (Yan et al., 2018), herbicidal (Duarte et al., 2022), anti-cancer (Coskun et al., 2017) and other biological activities (Li et al., 2018), in addition, chalcone has little toxic side effects. Compared with other natural products such as carvacrol and therapeutic, chalcone has the characteristics of simple synthesis (Aljelehawy et al., 2023, Alavi et al., 2023). Thus, chalcone is an important class of lead compounds on which compounds with excellent biological activity can be exploited.

In addition, pyridazine, also known as *o*-diazabenzene, is a class of nitrogen-containing heterocyclic compounds with a special structure and a wide range of biological activities. Pyridazine compounds exist with good biological activities in fungicides and pharmaceuticals (Fig. 1), such as anti-fungal (Cui et al., 2020, Dang et al., 2020), anti-bacterial (Mustafa and Mostafa 2020), herbicidal (Zou et al., 2017), insecticidal (Buysse et al., 2017), anti-viral (Galtier et al., 2003) and anti-cancer (Ahmed et al., 2021, He et al., 2021). Pyridazine is one of the more important active fragments in pesticides, and some commercial pyridazine pesticides have been successfully developed. Therefore, we introduced the pyridazine fragment.

Based on the considerations mentioned above and our continuing interest in developing high-efficiency, low-toxicity fungicides using the chalcone backbone, we envisaged a combination of the chalcone backbone and the pyridazine heterocycle to discover new fungicides. A series of chalcone derivatives containing pyridazine were designed, synthesized, and evaluated for their in vitro and in vivo antifungal activities against nine plant fungi and antibacterial activity against three plant bacteria. The compound B4, which possesses superior antifungal activity, was subjected to scanning electron microscopy, spore germination assay and in vivo antifungal assay to conduct a preliminary explore of its antifungal mechanism.

2. Materials and methods

2.1. Instruments and chemicals

^{1}H, ^{13}C, and ^{19}F nuclear magnetic resonance (NMR) spectra were obtained using Bruker Ascend 400 (Bruker Optics, Switzerland) and 500 MHz (Bruker Optics, Switzerland). High-resolution mass spectrometry (HRMS) data were conducted using a Thermo Scientific Q Exactive (Thermo Scientific, St. Louis, MO, U.S.A.). Scanning electronmicroscopy (SEM) data were obtained on FEI Nova Nano 450(Hillsboro, OR, U.S.A.). Microscope (Olympus Ltd, Japan). Melting point apparatus (Shanghai Yi Dian Physical Optics Instrument Co, Ltd, China).

2.2. Synthesis of target compounds

2.2.1. Synthesis of intermediates *1*

Intermediates **1** were synthesized by the reported methods (Zhou et al., 2022). Aqueous sodium hydroxide solution (5% NaOH, 5 mmol) was added to a round-bottomed flask containing 1-(4-hydroxyphenyl)ethan-1-one (4 mmol) and differently substituted aldehydes (6 mmol). The mixture was stirred at ambient temperature for 12 h. The resulting dark-yellow mixture was acidified by HCl (5% HCl, 5 mmol) after the reaction was completed. Finally, the mixture was filtered under vacuum, and the residue was dried to yield intermediate **1**.

2.2.2. Synthesis of intermediates *2*

Intermediates **2** were synthesized by the reported methods (Liu et al., 2017). Maleic hydrazide or phthalhydrazide (17.84 mmol) was added to $POCl_3$ or $POBr_3$ (30 mL), and the abovementioned mixture was heated to reflux for 2 h. After cooling to room temperature, add to a 250 mL ice bath beaker, decompress and filter to obtain the crude product, and rinse with clean water three times. Finally, recrystallize with DMF/water system to obtain intermediate **2**.

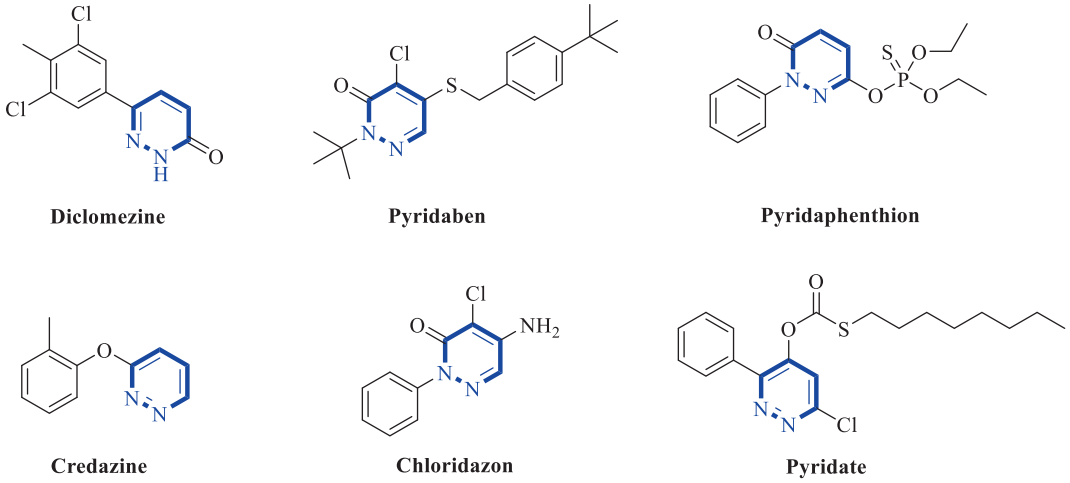

Fig. 1 The structures of some commercialized pyrimidine fungicides and herbicide.

2.2.3. Synthesis of *A1-A5*, *B1-B9* and *C1*

The intermediate **1** (1.93 mmol), intermediate **2** (2.32 mmol), and K_2CO_3 (5.80 mmol) were reacted in DMF for 5–8 h at 110 ℃, and the reaction was detected using TLC (Petroleum ether/ EtOAc = 1:1, *V*/*V*). After the reaction was completed, the system was poured into the water by cooling to room temperature, and the solid precipitated. The crude product was purified by column chromatography and eluted with (Petroleum ether/ EtOAc = 3:1, *V*/*V*) to give compounds **A1-A5**, **B1-B9**, and **C1**.

2.2.4. Synthesis of *D1-D5*

The target compound **B1-B5** (1.43 mmol) and sodium acetate (5.70 mmol) were poured into acetic acid (30 mL) and reacted at 110 ℃ for 5–6 h**.** Reaction detection by TLC (Petroleum ether/ EtOAc = 2:1, *V*/*V*). The crude product was purified by column chromatography and eluted with (Petroleum ether/ EtOAc = 3:1, *V*/*V*) to give compounds **D1-D5**.

The physical date, ^{1}H NMR, ^{13}C NMR, and ^{19}F NMR and HRMS data of the target compounds were provided in the Supporting Information.

2.3. Biological assays

2.3.1. Antibacterial activity in vitro

The in vitro anti-bacterial activities of target compounds **A1-A5**, **B1-B9**, **C1**, and **D1-D5** against the plant pathogenic bacteria *Xanthomonas oryzae pv. Oryzae* (*Xoo*), *Xanthomonas axonopodis pv. citri* (*Xac*) and *Pseudomonas syringae pv. actinidiae* (*Psa*) were evaluated by a slightly modified 96-well plate method(Moghaddam et al., 2014). Bismerthiazol (BT) and thiodiazole-copper (TC) were used as positive control agents.

2.3.2. Antifungal activity in vitro

The in vitro antifungal effects of the target compounds **A1-A5**, **B1-B9**, **C1**, and **D1-D5** against the plant pathogenic fungi *Rhizoctonia solani* (*RS*), *Botrytis cinerea* (*BC*), *Phomopsis* sp. (*PS*), *Colletotrichum acutatum* (*CA*), *Botryosphaeria dothicdea* (*Bd*), *Fusarium graminearum* (*FG*), *Colletotrichum gloeosporioides* (*CG*), *Sclerotinia sclerotiorum* (*SS*) and *Phytophthora capsica* (*PC*) were evaluated by a mycelial growth rate method (Wu et al., 2019, Long et al., 2021, Tian et al., 2021).

2.3.3. Antifungal activity in vivo

The in vivo biological activity of **B4** against *rice sheath blight disease* was determined by the reported in vitro leaf test and greenhouse experiments with slight modifications (Zhang et al., 2018) with the rice cultivar Fengyouxiangzhan. Azoxystrobin (AZ) was used as a positive control agent.

2.3.4. Spore germination assay

The inhibitory activity of **B4** on the spore germination of *B. cinerea* was assessed by microscopic observation. Spore suspensions (2×10^5 spores/mL) were prepared by seeding conidia in a 0.1% Tween 20 solution. The DMSO solution of the test compound **B4** was diluted with the conidial suspension to obtain five different final concentrations of 0, 25, 50, 100, and 200 μg/mL. Then, 30 μL of these cultures were removed to a concave slide and incubated in a humidity chamber at 28 °C and 90% relative humidity. Three replicates were performed, and a conidial suspension containing a corresponding concentration of acetone in water was regarded as the control. After incubation at 28 °C for 12 h, the number of germinated spores was examined by counting and measuring approximately 100 conidia in each field of three randomly selected fields under a biological microscope photographic system at 25 × magnification. The experiments were repeated three times. (Zhang et al., 2014).

2.3.5. Scanning electron microscopy (SEM)

To investigate in more detail the anti-bacterial and anti-fungal effects of the compounds, we used the Scanning electron microscopy (SEM) method reported in the literature (Peng et al., 2021, Tang et al., 2022).

2.3.6. Determination of MDA contents

Mycelia of *BC* were cultured on PDB medium on a rotary shaker (200 rpm) at 25 ℃. Then, prepared solutions of compound **B4** at different concentrations (0, 25, 50, 100 μg/mL) were

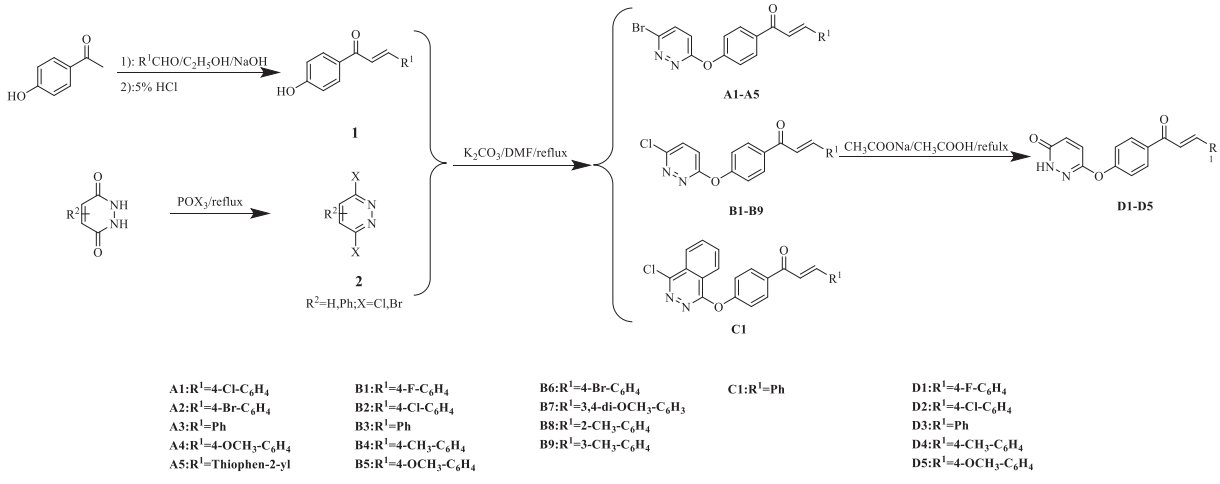

Scheme 1 Synthetic route of the target compounds.

Table 1 Antibacterial activity of Target Compounds *in vitro*[a].

Compd.	*Xac* (%)		*Psa* (%)		*Xoo* (%)	
	100 μg/mL	50 μg/mL	100 μg/mL	50 μg/mL	100 μg/mL	50 μg/mL
A1	16.99 ± 2.57	15.07 ± 1.59	8.52 ± 0.85	7.83 ± 0.06	12.37 ± 4.19	10.48 ± 3.41
A2	34.15 ± 1.11	15.76 ± 1.13	10.06 ± 0.45	7.92 ± 0.10	18.56 ± 1.04	17.59 ± 1.24
A3	6.76 ± 0.72	5.96 ± 2.21	7.10 ± 0.87	6.10 ± 0.81	6.39 ± 6.10	4.09 ± 1.16
A4	35.66 ± 4.76	15.39 ± 0.76	14.34 ± 0.53	12.07 ± 0.15	35.43 ± 1.20	14.80 ± 2.74
A5	32.32 ± 3.94	15.34 ± 3.96	11.16 ± 0.98	9.70 ± 0.87	16.62 ± 0.96	15.49 ± 7.39
B1	10.26 ± 3.54	3.84 ± 4.16	14.62 ± 0.17	9.34 ± 0.32	16.16 ± 1.57	10.38 ± 0.12
B2	24.05 ± 1.86	23.57 ± 1.19	10.84 ± 0.42	8.20 ± 0.56	23.72 ± 0.49	19.02 ± 0.60
B3	15.07 ± 2.76	13.52 ± 4.72	12.80 ± 3.15	10.20 ± 0.49	9.41 ± 2.28	4.70 ± 0.12
B4	24.00 ± 1.80	13.95 ± 1.50	7.79 ± 0.79	5.56 ± 0.61	40.34 ± 0.26	36.91 ± 0.84
B5	24.80 ± 4.74	17.48 ± 3.88	8.70 ± 0.57	8.42 ± 1.21	9.36 ± 6.26	4.34 ± 0.41
B6	42.40 ± 1.15	6.78 ± 10.1	8.14 ± 0.31	8.10 ± 0.66	22.91 ± 0.59	21.03 ± 0.15
B7	16.19 ± 1.25	8.76 ± 1.53	7.29 ± 4.52	5.37 ± 0.99	11.61 ± 1.85	9.97 ± 0.10
B8	55.66 ± 3.35	23.89 ± 2.42	10.56 ± 1.36	9.56 ± 0.59	41.24 ± 0.56	20.49 ± 0.79
B9	9.72 ± 1.87	4.04 ± 1.13	6.29 ± 0.36	4.16 ± 1.04	28.51 ± 1.08	12.88 ± 3.26
C1	18.81 ± 0.46	17.21 ± 1.08	10.20 ± 0.31	8.29 ± 0.40	15.64 ± 2.46	12.32 ± 4.13
D1	33.04 ± 0.76	25.23 ± 5.54	21.45 ± 1.35	16.12 ± 1.10	26.07 ± 1.93	24.62 ± 2.60
D2	29.72 ± 6.62	22.02 ± 7.86	14.77 ± 0.89	10.70 ± 0.78	35.66 ± 1.31	29.50 ± 2.11
D3	35.07 ± 3.22	32.08 ± 8.55	8.48 ± 0.06	7.91 ± 0.86	36.35 ± 0.70	34.59 ± 1.10
D4	47.59 ± 0.95	15.71 ± 4.86	16.62 ± 2.74	11.46 ± 0.91	27.68 ± 0.53	24.11 ± 0.70
D5	50.64 ± 2.60	33.25 ± 4.48	13.07 ± 0.75	9.47 ± 1.06	22.28 ± 2.36	21.16 ± 1.14
TC[b]	63.36 ± 5.57	44.35 ± 8.46	69.34 ± 0.86	35.98 ± 0.46	63.25 ± 3.23	39.76 ± 2.70
BT[b]	51.68 ± 6.63	45.21 ± 2.92	51.91 ± 1.27	35.30 ± 0.66	49.44 ± 2.36	43.53 ± 1.06

[b] TC (thiodiazole copper) and BT (bismerthiazol).

Table 2 EC_{50} of Target Compound **B8** against *Xac*.[a]

Compd.	EC_{50} (μg/mL)	r^2	Regression equation
B8	78.89	0.9745	y = 1.5652x + 2.0308
TC[b]	70.43	0.9848	y = 2.0721x + 1.1713
BT[b]	86.72	0.9892	y = 1.9458x + 1.2288

[a] Average of three trials.
[b] TC (thiodiazole copper) and BT (bismerthiazol).

added and incubated with the mycelia for 24 h at 25 °C. The medium was filtered, and the hyphae were collected in a vacuum freeze dryer. Mycelia (0.1 g) were homogenized in an ice bath with 1 mL of MDA extract (produced by Solarbio Technology Co., Ltd., Beijing, China) and centrifuged at 8000 g and four °C for 15 min. The supernatant was removed, added to each reagent according to the kit instructions, held in a 100 °C water bath for 60 min, cooled in an ice bath, and centrifuged at 10,000 g for 10 min at room temperature. The supernatant was aspirated, and then the absorbance of each sample was measured at 532 nm and 600 nm. Each group was repeated three times. MDA content in mycelia was determined using an MDA assay kit (Beijing Solarbio Science & Technology Co.) (Mo et al., 2021).

3. Results and discussion

3.1. Chemistry

As shown in Scheme 1, compounds **A1-A5**, **B1-B9**, **C1** and **D1-D5** were synthesized, and characterized their structures by ^{1}H NMR, ^{13}C NMR, ^{19}F NMR and HRMS. All synthetic compounds were original.

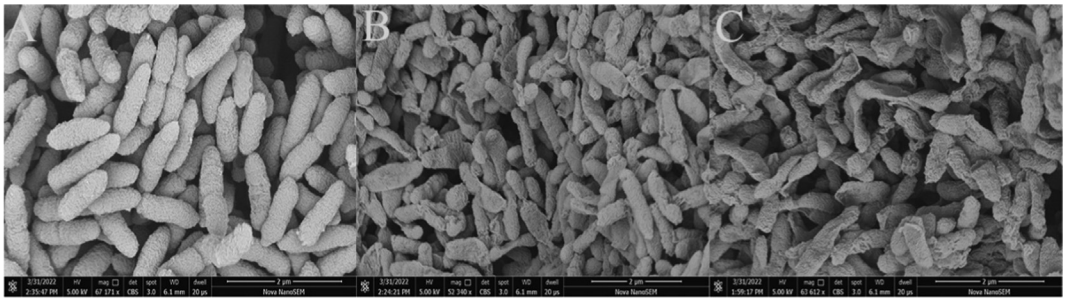

Fig. 2 Scanning electron micrographs of *Xac* in the presence of different concentrations of **B8** (A) 0 μg/mL; (B) 50 μg/mL and (C) 100 μg/mL. Scale bar for (A, B and C) are 2 μm.

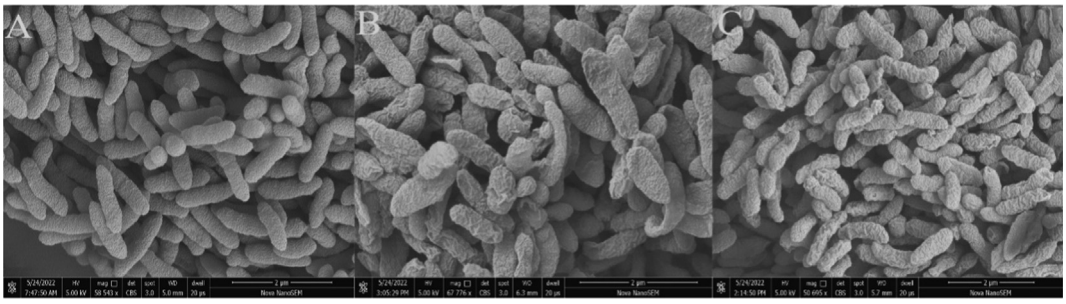

Fig. 3 Scanning electron micrographs of *Xoo* in the presence of different concentrations of **B4** (A) 0 μg/mL; (B) 50 μg/mL and (C) 100 μg/mL. Scale bar for (A, B and C) are 2 μm.

Table 3 Inhibition effect of target compounds against nine plant phytopathogenic fungi at 100 μg/mL.[a]

Compd.	*BC*	*PS*	*CG*	*CA*	*RS*	*PC*	*SS*	*BD*	*FG*
A1	20.53 ± 3.36	35.06 ± 2.68	21.25 ± 4.14	0.00 ± 0.00	53.70 ± 3.27	15.28 ± 2.32	42.13 ± 1.32	38.60 ± 3.80	0.00 ± 0.00
A2	22.81 ± 4.19	39.85 ± 1.67	37.92 ± 2.94	0.00 ± 0.00	59.26 ± 1.81	18.98 ± 1.13	39.57 ± 3.09	23.53 ± 1.14	17.74 ± 3.60
A3	34.22 ± 3.03	55.72 ± 0.00	27.08 ± 5.84	16.97 ± 1.67	49.63 ± 3.04	36.11 ± 1.76	50.64 ± 2.08	9.40 ± 2.21	9.06 ± 1.66
A4	22.05 ± 3.93	38.75 ± 3.33	22.50 ± 6.26	5.50 ± 2.29	59.63 ± 0.91	30.09 ± 1.13	41.28 ± 3.23	26.47 ± 2.28	11.32 ± 3.25
A5	20.15 ± 6.92	40.22 ± 1.98	32.08 ± 7.46	0.00 ± 0.00	52.96 ± 0.91	27.31 ± 1.13	49.36 ± 1.92	0.00 ± 0.00	21.89 ± 3.62
B1	36.12 ± 1.44	52.40 ± 7.51	39.58 ± 2.18	12.84 ± 1.14	56.30 ± 1.15	26.39 ± 1.52	47.23 ± 2.08	36.40 ± 8.65	35.09 ± 1.14
B2	22.81 ± 0.93	43.54 ± 2.32	42.92 ± 5.13	0.00 ± 0.00	55.19 ± 0.91	14.35 ± 1.13	49.79 ± 1.32	6.71 ± 3.34	32.83 ± 1.14
B3	41.44 ± 2.76	52.03 ± 2.68	37.08 ± 6.68	25.23 ± 1.67	31.48 ± 0.91	37.50 ± 1.52	45.96 ± 1.92	25.37 ± 3.25	32.83 ± 4.97
B4	100 ± 0.00	82.66 ± 1.67	48.75 ± 3.64	51.83 ± 1.21	85.67 ± 1.67	35.65 ± 1.13	75.74 ± 2.14	11.41 ± 2.55	65.66 ± 0.90
B5	25.10 ± 4.94	47.23 ± 1.67	22.50 ± 2.80	22.48 ± 3.26	57.41 ± 1.67	29.17 ± 1.52	42.13 ± 2.64	25.00 ± 3.95	22.26 ± 1.80
B6	31.94 ± 3.93	42.07 ± 2.59	22.50 ± 5.42	0.92 ± 1.40	57.04 ± 1.15	13.89 ± 1.76	40.85 ± 2.51	12.75 ± 9.06	1.51 ± 1.21
B7	32.32 ± 8.62	46.13 ± 4.57	28.75 ± 3.05	11.93 ± 4.43	47.04 ± 1.67	36.57 ± 2.09	45.53 ± 1.32	22.43 ± 1.66	35.85 ± 1.14
B8	12.17 ± 2.79	45.76 ± 1.21	25.42 ± 3.55	0.00 ± 0.00	25.10 ± 2.08	8.80 ± 2.73	16.23 ± 2.98	0.00 ± 0.00	16.98 ± 2.28
B9	24.71 ± 4.20	45.39 ± 3.33	24.58 ± 2.94	0.00 ± 0.00	24.69 ± 2.68	12.50 ± 2.32	15.79 ± 1.61	0.00 ± 0.00	18.49 ± 6.54
C1	37.26 ± 1.25	70.11 ± 1.85	26.67 ± 4.35	38.53 ± 1.14	58.52 ± 1.81	29.17 ± 1.52	39.57 ± 3.09	12.75 ± 4.16	13.96 ± 3.69
D1	52.85 ± 1.86	53.14 ± 3.26	39.17 ± 5.72	29.36 ± 3.88	55.19 ± 1.67	43.98 ± 1.13	48.94 ± 1.61	18.79 ± 3.03	20.75 ± 0.00
D2	45.68 ± 2.89	59.78 ± 0.90	40.00 ± 1.40	11.47 ± 1.67	62.59 ± 0.91	44.44 ± 1.76	56.60 ± 1.61	20.13 ± 4.71	6.04 ± 1.85
D3	44.19 ± 3.36	57.93 ± 2.43	36.67 ± 4.45	47.71 ± 3.13	62.22 ± 1.41	42.59 ± 1.43	60.85 ± 2.64	0.00 ± 0.00	21.89 ± 1.85
D4	40.30 ± 3.03	46.86 ± 3.43	31.25 ± 6.06	5.96 ± 3.55	59.26 ± 1.15	32.41 ± 1.43	48.09 ± 2.08	18.12 ± 2.08	8.68 ± 5.86
D5	37.26 ± 3.46	40.96 ± 3.02	30.83 ± 2.68	2.29 ± 1.21	57.78 ± 1.41	29.17 ± 2.32	44.26 ± 3.39	5.37 ± 5.55	3.77 ± 2.31
AZ[b]	87.45 ± 1.25	91.51 ± 1.67	63.33 ± 4.12	73.85 ± 1.21	76.30 ± 1.15	60.65 ± 4.78	88.51 ± 3.13	79.04 ± 2.31	66.79 ± 1.14

[a] Average of three trials.
[b] AZ (Azoxystrobin).

3.2. Antibacterial activity

3.2.1. Antibacterial activity in vitor

The antibacterial effects of target compounds against *Xac*, *Xoo*, and *Psa* were detected by the turbidimetric method, as shown in Table 1. The against *Xac* activity of **B8** (55.7%) at 100 μg/mL was superior to **BT** and slightly lower than **TC**.

The EC_{50} values of **B8** against *Xac* was further measured according to the method mentioned above (Table 2). From the data, the EC_{50} value of **B8** (EC_{50} = 78.89 μg/mL) was excellent than **BT** (EC_{50} = 86.72 μg/mL) and approaching **TC** (EC_{50} = 70.43 μg/mL).

The structure–activity relationship (SAR) was analyzed on the basis of the antibacterial activities against *Xac*, *Xoo*, and *Psa*, shown in Table 1. When R_1 was the Ph group, the antibacterial activity was **A3** < **B3** < **C1** < **D4**. When R_1 was an electron-donating group, such as the 4-OCH_3-Ph group, the antibacterial activity was **B5** < **A4** < **D5**. When R_1 was an electron-absorbing group such as the 4-F-Ph group, the antibacterial activity was **B1** < **D1**. When R_1 was CH_3-Ph group, the antibacterial activity was **B9** < **B4** < **B8**.

3.2.2. Scanning electron microscopy

We further investigated the mechanism of action of **B8** on *Xac* and **B4** on *Xoo* by scanning electron microscopy. As shown in Fig. 2, when the concentration of **B8** was 0 μg/mL (A), the *Xac* cells were fully packed, and the surface was smooth; when the concentration of **B8** was 50 μg/mL (B), a few *Xac* cells showed a certain degree of fold and flattening on the surface of the cell membrane. When the concentration increased to 100 μg/mL

(C), many *Xac* cells showed flattening on the surface of the cell membrane, and the folded condition increased, eventually leading to cell death.

The effect of different concentrations of drugs interacting with *Xac* can be seen in Fig. 3. At a concentration of 0 μg/mL (A), all *Xac* cells are full and have a smooth surface. At a concentration of 50 μg/mL (B), a few *Xac* cells showed a certain degree of ruffling and flattening. When the concentration was increased to 100 μg/mL (C), a large number of *Xac* cells showed flattened surface, and the folded condition increased, but no membrane damage occurred. Compared to compound **B8**, **B4** does not cause cell membrane damage, resulting in cell death.

3.3. Antifungal activity

3.3.1. Antifungal activity in vitro

According to the results of antifungal activity evaluation (Table 3), chalcone derivatives **A1-A5**, **B1-B9**, **C1**, and **D1-D5** were screened against nine plant fungi (*RS*, *BC*, *PS*, *CA*, *FG*, *CG*, *SS*, *PC*, *BD*) at 100 μg/mL. The mycelial growth inhibition assay was used to determine the inhibition of the target compounds against the nine fungi at a concentration of 100 μg/mL. The data in Table 3 showed that some of the target compounds had excellent antifungal activity. Among them, **B4** showed excellent inhibitory activity against most of the tested

Table 4 The EC_{50} values of the part of target compound against Fungicidal Activities.[a]

Fungi	Compd	EC_{50} (μg/mL)	r^2	Regression equation
BC	**B4**	8.91	0.9889	y = 2.3932x + 2.7194
	AZ	20.28	0.9453	y = 1.0088x + 3.9899
RS	**B4**	18.10	0.9443	y = 1.2111x + 3.4755
	D2	20.18	0.9767	y = 0.7602x + 4.0080
	D3	20.60	0.9289	y = 0.8345x + 3.9036
	AZ	10.23	0.9417	y = 0.9366x + 4.0541
SS	**B4**	20.62	0.9404	y = 0.7288x + 4.0421
	AZ	17.46	0.9394	y = 0.8942x + 3.8893
PS.	**B4**	20.82	0.9774	y = 1.2576x + 3.3440
	AZ	10.67	0.9637	y = 0.5070x + 4.4788

[a] Average of three trials.

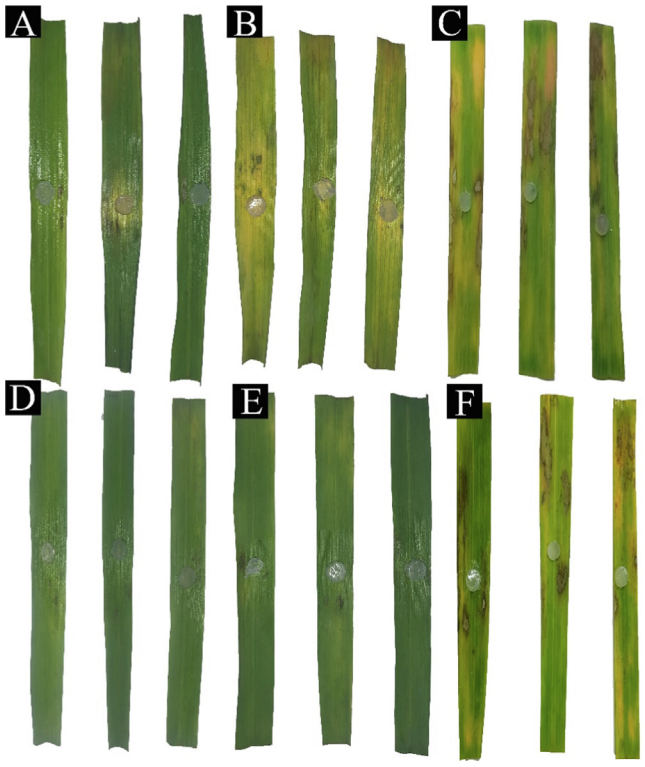

Fig. 4 The protective efficacy of **B4** against rice sheath blight on detached rice leaves, (A) **B4** at 200 μg/ mL; (B) **B4** at 100 μg/ mL; (C) Control, 0.1% DMSO; (D) AZ at 200 μg/ mL; (E) AZ at 100 μg/ mL; (F) Negative control.

fungi and was superior to the AZ (87.45% and 76.30%) at 100 μg/mL concentration against *BC* (100%) and *RS* (85.67%) and close to the AZ against *PS* (82.66%), *SS* (75.74%), and *FG* (65.66%). To further determine the activity of the target compounds, we performed EC_{50} determination of the target compounds, which is shown in Table 4. From Table 4, we know that the EC_{50} values of **B4** against *BC* and *RS* were 8.91 μg/mL and 18.10 μg/mL better than the AZ, and the EC_{50} values of **D2** and **D3** were 20.18 μg/mL and 20.60 μg/mL and comparable to AZ. Therefore, we selected *BC* and *RS* for the mechanism study.

3.3.2. *Antifungal activity in vivo*

In order to further examine the application prospect of the potent **B4**, its' protective activity and curative activity against *RS* were first measured by the detached leaf assay in vivo. As shown in Fig. 4, Fig. 5 and Table 5, the obtained experimental results indicated **B4** could significantly inhibit *RS* growth. Fig. 4 shows the control (C) and negative control (F) rice leaves with large spot lengths and yellowing leaves. The rice leaves treated with **B4** (A) at 200 μg/mL (63.15%) had shorter spot lengths and greener leave colours, which were close to the AZ (66.53%). As shown in Fig. 5, the rice leaves treated with

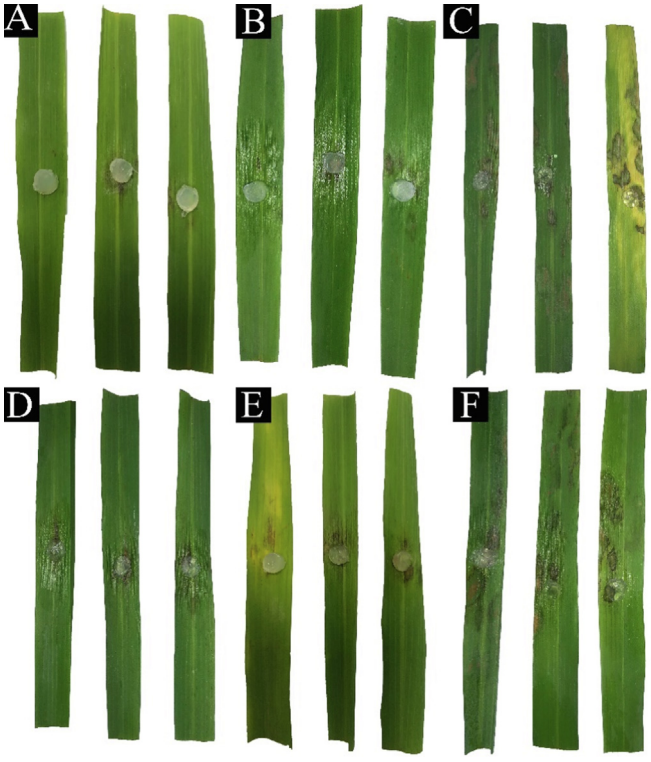

Fig. 5 The Curative efficacy of **B4** against rice sheath blight on detached rice leaves (A) **B4** at 200 μg/mL; (B) **B4** at 100 μg/mL; (C) control, 0.1% DMSO; (D) AZ at 200 μg/mL; (E) AZ at 100 μg/mL; (F) Negative control.

Table 5 The control efficacy against rice sheath blight disease of **B4** on rice leaves.[a]

Treatment	Concentration(μg/mL)	Curative activity		Protective activity	
		Lesion length (cm)	Control efficacy (%)	Lesion length (cm)	Control efficacy (%)
B4	100	2.20 ± 0.45	67.35	3.86 ± 0.28	44.05
	200	0.89 ± 0.42	86.85	2.54 ± 0.24	63.15
AZ	100	2.12 ± 0.55	68.41	3.79 ± 0.25	45.06
	200	1.45 ± 0.34	78.38	2.31 ± 0.30	66.53
Negative control		6.74 ± 0.44	–	7.23 ± 0.56	–

[a] Values are the average of 10 replicates.

B4 (A) at 200 μg/mL (with an impressive curative efficacy of 86.85%) had a shooter spot length, which was better than AZ (78.38%). The curative activity of **B4** (B) at 100 μg/mL was 67.35%, which was slightly lower than that of the AZ (68.41%), but there was still a significant quality effect compared to the control (C) and negative control (F). Therefore, these experiments indicated that **B4** could effectively control rice sheath blight disease caused by *RS*.

3.3.3. Spore germination assay

The target compound **B4** was assayed against in-spore germination of *BC* at concentrations of 0, 25, 50, 100, and 200 μg/mL. *BC* infects hosts through RNA disruption of plant defence mechanisms with the help of conidia so that **B4** can reduce damage to host plants by inhibiting spore germination. As shown in Fig. 6 and Fig. 7**, B4** effectively inhibited spore germination in a concentration-dependent manner. As shown in Fig. 6, the spores in the control group (A) all germinated. But the number of spores germinated began to decrease when the concentration of compound **B4** increased. Only half the spores germinate when **B4** (B) at 25 μg/mL, while when the concentration rises to 100 μg/mL (D), only one tenth of the spores germinate, with a significant increase in the inhibition rate. When **B4** (F) at 200 μg/mL, the relative inhibition of spore germination was 100%. As shown in Fig. 7, the relative inhibition of spore germination was 100, 90.77, 72.58 and 51.51% at concentrations of 200, 100, 50 and 25 μg/mL, respectively. The EC_{50} value of **B4** was 26.55 μg/mL, indicating a good inhibition rate against the spores. In contrast to the mycelium inhibition experiment, the inhibition rate of **B4** on spore germination was lower than on mycelium, indicating that the compound inhibited mycelium better.

*3.3.4. Phospholipid peroxidation of BC induced by **B4***

Malondialdehyde (MDA) is a critical metabolic executive in the peroxidation process of biological cell membranes and can also reflect the extent of damage to cell membranes by oxidative stress. After the effect of **B4** Fig. 8, the MDA content increased with increasing concentration and was 1.83, 2.05 and 2.41 times higher than that of the control when the concentration of **B4** was 25, 50, and 100 μg/mL, respectively. Therefore, it can be shown that **B4** can significantly increase the degree of lipid peroxidation of *BC* cell membrane, and the degree of lipid peroxidation was positively correlated with the concentration of the compound.

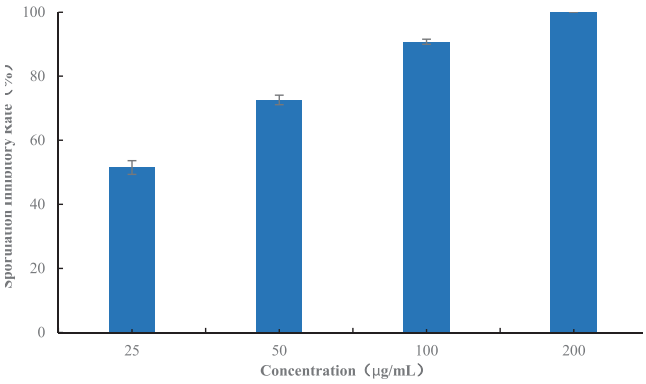

Fig. 7 *In vitro* effect of **B4** against spore germination of *BC*.

*3.3.5. Effect of compound **B4** on the hyphae morphology of BC*

As shown in Fig. 9, scanning electron microscopy revealed that the mycelium of the blank control group had normal morphology, uniform thickness, smooth surface and good growth. In

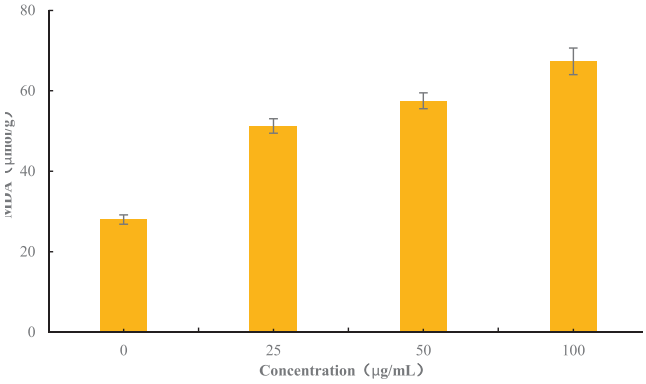

Fig. 8 MDA contents of *BC* treated with **B4.**

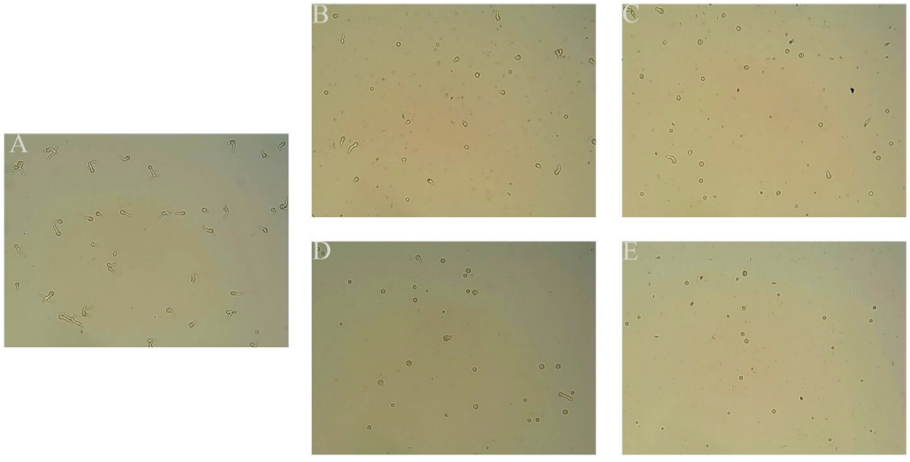

Fig. 6 Effects of **B4** on spore germination of *BC* (A) 0 μg/mL; (B)25 μg/mL; (C) 50 μg/mL; (D) 100 μg/mL and (E) 200 μg/mL.

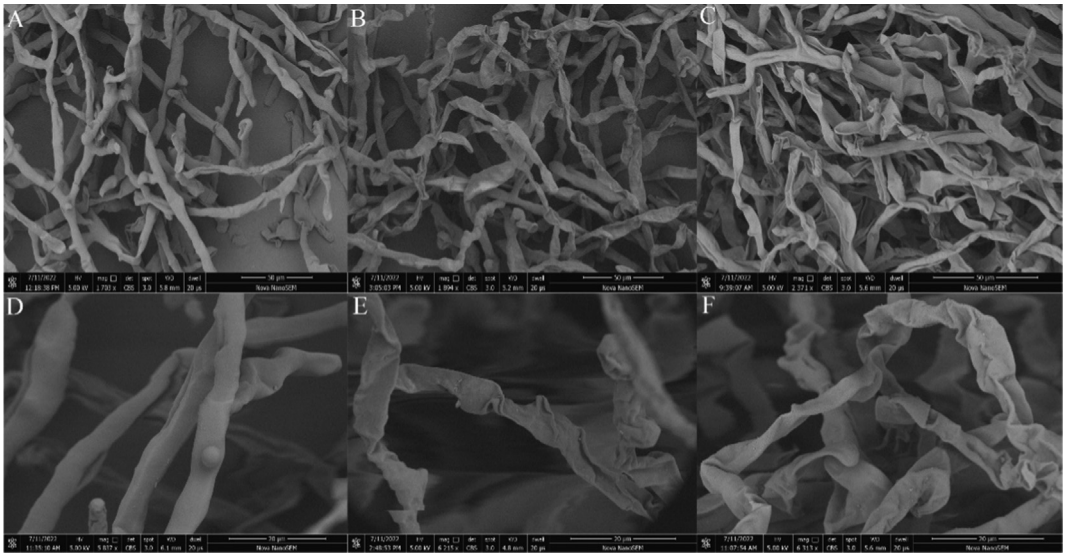

Fig. 9 Scanning electron micrographs of *BC* mycelia. (A,D) negative control, 0.1% DMSO; (B,E) treated with 0.1% DMSO plus **B4** at 50 μg/mL; (C,F) treated with 0.1% DMSO plus **B4** at 100 μg/mL; Scale bar for (A, B and C) are 50 μm. Scale bar for (D, E and F) are 20 μm.

contrast, after 50 μg/mL and 100 μg/mL **B4** treatment, the mycelium was wrinkled, collapsed, severely deformed and varied in thickness. Therefore, **B4** can destroy the morphology of the mycelium of *BC*, thus affecting the average growth of mycelium.

4. Conclusion

In summary, a series of chalcone derivatives containing pyridazine moiety had been designed and synthesized and their structures had been identified by NMR and HRMS. All the target compounds were assayed for their biological activities against three bacteria and nine fungi. The results showed excellent antibacterial and antifungal activities for some of the target compounds. Antibacterial activities result show **B8** possessed the best bacterial activity with an EC_{50} value of 78.89 μg/mL against *Xac*, which was superior to BT (EC_{50} = 86.72 μg/mL). Antifungal activities result show **B4** at 100 μg/mL concentration showed excellent inhibitory activity against most of the tested fungi and was superior to the AZ (87.45% and 76.30%) against *BC* (100%) and *RS* (85.67%). In vivo protective activity and curative activity against *RS* of **B4** results indicated that compound **B4** was able to significantly inhibit rice sheath blight disease, having a curative efficacy of 86.85% at 200 μg/mL. Scanning electron microscopy, spore germination assay and phospholipid peroxidation assay were taken for the preliminary study of the antifungal mechanism. Scanning electron microscopy and phospholipid peroxidation assay results showed that **B4** could destroy the hyphal morphology of *BC* and affect cell membrane permeability. Spore germination assay results showed that **B4** could effectively inhibit spore germination of *BC*. In short, the present work implied that **B4** could be regarded as promising candidate for developing more effective fungicides to fight against the pathogen *BC*.

Declaration of Competing Interest

The authors declare that they have no known competing financial interests or personal relationships that could have appeared to influence the work reported in this paper.

Acknowledgements

This research was completed with the support of the National Natural Science Foundation of China (No. 32072446), the Science Foundation of Guizhou Province (No. 20192452).

Appendix A. Supplementary data

Supplementary data to this article can be found online at https://doi.org/10.1016/j.arabjc.2023.104852.

References

Ahmed, M.F., Santali, E.Y., El-Deen, E.M., Naguib, I.A., El-Haggar, R., 2021. Development of pyridazine derivatives as potential EGFR inhibitors and apoptosis inducers: Design, synthesis, anticancer evaluation, and molecular modeling studies. Bioorg. Chem. 106, 104473.

Alavi, M., Yarani, R., Sreedharan, M., Thomas, S., 2023. Micro and nanoformulations of catechins for therapeutic applications: recent advances and challenges. Micro Nano Bio Aspects. 2 (1), 8–19.

Aljelehawy, Q., Maroufi, Y., Javid, H., Mohammadi, M.R., Raji Mal Allah, O., Taheri, S.V., Mohammadzade, H., 2023. Anticancer, antineurodegenerative, antimicrobial, and antidiabetic activities of carvacrol: recent advances and limitations for effective formulations. Nano Micro Biosystems. 2 (1), 1–10.

Buysse, A.M., Yap, M.C., Hunter, R., Babcock, J., Huang, X., 2017. Synthesis and biological activity of pyridazine amides, hydrazones and hydrazides. Pest. Manage. Sci. 73 (4), 782–795.

Coskun, D., Erkisa, M., Ulukaya, E., Coskun, M.F., Ari, F., 2017. Novel 1-(7-ethoxy-1-benzofuran-2-yl) substituted chalcone derivatives: Synthesis, characterization and anticancer activity. Eur. J. Med. Chem. 136, 212–222.

Cui, Z.M., Zhou, B.H., Fu, C., Chen, L., Fu, J., Cao, F.J., Yang, X.J., Zhou, L., 2020. Simple Analogues of Quaternary Benzo[c]phenanthridine Alkaloids: Discovery of a Novel Antifungal 2-Phenylphthalazin-2-ium Scaffold with Excellent Potency against Phytopathogenic Fungi. J Agric Food Chem. 68 (52), 15418–15427.

Dang, M.M., Liu, M., Huang, L., Ou, X.M., Long, C., Liu, X.Y., Ren, Y., Zhang, P., Huang, M.Z., Liu, A.P., 2020. Design, synthesis, and bioactivities of novel pyridazinone derivatives containing 2-phenylthiazole or oxazole skeletons. J. Heterocycl. Chem. 57 (11), 4088–4098.

Dean, R., Van Kan, J.A., Pretorius, Z.A., Hammond-Kosack, K.E., Di Pietro, A., Spanu, P.D., Rudd, J.J., Dickman, M., Kahmann, R., Ellis, J., Foster, G.D., 2012. The Top 10 fungal pathogens in molecular plant pathology. Mol. Plant Pathol. 13 (4), 414–430.

Dkhar, L., Banothu, V., Pinder, E., Phillips, R.M., Kaminsky, W., Kollipara, M.R., 2020. Ru, Rh and Ir metal complexes of pyridyl chalcone derivatives: Their potent antibacterial activity, comparable cytotoxicity potency and selectivity to cisplatin. Polyhedron 185, 114606.

Duarte, V.S., Paula, R.L., Custodio, J.M., D'Oliveira, G.D., Borges, L.L., Perez, C.N., Perjesi, P., Oliver, A.G., Napolitano, H.B., 2022. A new quinolinone-chalcone hybrid with potential antibacterial and herbicidal properties using in silico approaches. J. Mol. Model. 28 (6), 176.

Funakoshi-Tago, M., Okamoto, K., Izumi, R., Tago, K., Yanagisawa, K., Narukawa, Y., Kiuchi, F., Kasahara, T., Tamura, H., 2015. Anti-inflammatory activity of flavonoids in Nepalese propolis is attributed to inhibition of the IL-33 signaling pathway. Int. Immunopharmacol. 25 (1), 189–198.

Galtier, C., Mavel, S., Snoeck, R., Andreï, G., Pannecouque, C., Witvrouw, M., Balzarini, J., De Clercq, E., Gueiffier, A., 2003. Synthesis and Antiviral Activities of 3-Aralkyl-Thiomethylimidazo[1,2-b]Pyridazine Derivatives. Antiviral Chem. Chemother. 14, 177–182.

Gan, X.H., Hu, D.Y., Wang, Y.J., Yu, L.S., Song, B.A., 2017. Novel trans-Ferulic Acid Derivatives Containing a Chalcone Moiety as Potential Activator for Plant Resistance Induction. J. Agric. Food. Chem. 65 (22), 4367–4377.

He, Z.X., Gong, Y.P., Zhang, X., Ma, L.Y., Zhao, W., 2021. Pyridazine as a privileged structure: An updated review on anticancer activity of pyridazine containing bioactive molecules. Eur. J. Med. Chem. 209, 112946.

Li, H., Chen, Y., Z, Z, Q., Li, B, Q., G, Z., Tian, S, P., 2018. Pathogenic mechanisms and control strategies of Botrytis cinerea causing post-harvest decay in fruits and vegetables. Food Qual. Saf. 2(3), 111-119.

Li, J.F., Li, D., Xu, Y.M., Guo, Z.B., Liu, X., Yang, H., Wu, L.C., Wang, L.S., 2018b. Design, synthesis, biological evaluation, and molecular docking of chalcone derivatives as anti-inflammatory agents. Bioor. Med. Chem Lett. 27 (3), 602–606.

Liu, J.C., Chen, M., Wang, Y.L., Zhao, X.Y., Wang, S.J., Wu, Y.L., Zhang, W., 2017. Synthesis and the interaction of 2-(1*H*-pyrazol-4-yl)-1*H*-imidazo[4,5-f][1,10]phenanthrolines with telomeric DNA as lung cancer inhibitors. Eur. J. Med. Chem. 133, 36–49.

Long, Z.Q., Yang, L.L., Zhang, J.R., Liu, S.T., Xie, J., Wang, P.Y., Zhu, J.J., Shao, W.B., Liu, L.W., Yang, S., 2021. Fabrication of Versatile Pyrazole Hydrazide Derivatives Bearing a 1,3,4-Oxadiazole Core as Multipurpose Agricultural Chemicals against Plant Fungal, Oomycete, and Bacterial Diseases. J. Agric. Food. Chem. 69 (30), 8380–8393.

Lu, A.D., Wang, J.J., Liu, T.J., Han, J., Li, Y.H., Su, M., Chen, J.X., Zhang, H., Wang, L.Z., Wang, Q.M., 2014. Small Changes Result in Large Differences: Discovery of (-)-Incrustoporin Derivatives as Novel Antiviral and Antifungal Agents. J. Agric. Food. Chem. 62 (35), 8799–8807.

Ma, D.C., Jiang, J.G., He, L.M., Cui, K.D., Mu, W., Liu, F., 2018. Detection and Characterization of Qol-Resistant Phytophthora capsici Causing Pepper Phytophthora Blight in China. Plant Dis. 102 (9), 1725–1732.

Mo, F.X., Hu, X.F., Ding, Y., Li, R.Y., Long, Y.H., Wu, X.M., Li, M., 2021. Naturally produced magnolol can significantly damage the plasma membrane of Rhizoctonia solani. Pestic. Biochem. Physiol. 178, 104942.

Moghaddam, M., Alymanesh, M.R., Mehdizadeh, L., Mirzaei, H., Ghasemi Pirbalouti, A., 2014. Chemical composition and antibacterial activity of essential oil of Ocimum ciliatum, as a new source of methyl chavicol, against ten phytopathogens. Ind. Crops Prod. 59, 144–148.

Muller, R., Shinn, C., Waldvogel, A.M., Oehlmann, J., Ribeiro, R., Moreira-Santos, M., 2019. Long-term effects of the fungicide pyrimethanil on aquatic primary producers in macrophyte-dominated outdoor mesocosms in two European ecoregions. Sci. Total Environ. 665, 982–994.

Mustafa, M., Mostafa, Y.A., 2020. Antimicrobial Pyridazines: Synthesis, Characterization, Cytotoxicity, Promiscuity, and Molecular Docking. Chem. Biodivers. 17, 6.

Peng, F., Liu, T.T., Wang, Q.F., Liu, F., Cao, X., Yang, J.S., Liu, L. W., Xie, C.W., Xue, W., 2021. Antibacterial and Antiviral Activities of 1,3,4-Oxadiazole Thioether 4*H*-Chromen-4-one Derivatives. J. Agric. Food. Chem. 69 (67), 11085–11094.

Shasmita, Mohapatra, D., Mohapatra, P.K., Naik, S.K., Mukherjee, A. K., 2019. Priming with salicylic acid induces defense against bacterial blight disease by modulating rice plant photosystem II and antioxidant enzymes activity. Physiol. Mol. Plant Pathol. 108, 101427.

Silva, R.N., Monteiro, V.N., Steindorff, A.S., Gomes, E.V., Noronha, E.F., Ulhoa, C.J., 2019. Trichoderma/pathogen/plant interaction in pre-harvest food security. Fungal Biol. 123, 565–583.

Tang, X.M., Zhan, W.L., Chen, S., Zhou, R., Hu, D., Sun, N., Fei, Q., Wu, W.N., Xue, W., 2022. Synthesis, bioactivity and preliminary mechanism of action of novel trifluoromethyl pyrimidine derivatives. Arabian J. Chem. 15, (9) 104110.

Tian, Z.Y., Liao, A.C., Kang, J., Gao, Y.Y., Lu, A.L., Wang, Z.W., Wang, Q.M., 2021. Toad Alkaloid for Pesticide Discovery: Dehydrobufotenine Derivatives as Novel Agents against Plant Virus and Fungi. J. Agric. Food. Chem. 69 (34), 9754–9763.

Tomar, V., Bhattacharjee, G., Kamaluddin, N., Rajakumar, S., Srivastava, K., Puri, S.K., 2009. Synthesis of new chalcone derivatives containing acridinyl moiety with potential antimalarial activity. Eur. J. Med. Chem. 45 (2), 745–751.

Williamson, B., Tudzynski, B., Tudzynski, P., van Kan, J.A., 2007. Botrytis cinerea: the cause of grey mould disease. Mol. Plant Pathol. 8 (5), 561–580.

Wu, S.K., Shi, J., Chen, J.X., Hu, D.Y., Zang, L.S., Song, B.A., 2021. Synthesis, Antibacterial Activity, and Mechanisms of Novel 6-Sulfonyl-1,2,4-triazolo 3,4-b 1,3,4 thiadiazole Derivatives. J. Agric. Food. Chem. 69 (16), 4645–4654.

Wu, Y.Y., Shao, W.B., Zhu, J.J., Long, Z.Q., Liu, L.W., Wang, P.Y., Li, Z., Yang, S., 2019. Novel 1,3,4-Oxadiazole-2-carbohydrazides as Prospective Agricultural Antifungal Agents Potentially Targeting Succinate Dehydrogenase. J. Agric. Food. Chem. 67 (50), 13892–13903.

Yan, Y.K., Xu, Q., Gao, Y., Liu, H., Tang, X.R., 2018. Synthesis and Study on Insecticidal Activity of New Heterocyclic Chalcone Derivatives. Chin. J. Org. Chem. 38 (7), 1763–1771.

Zhang, J., Yan, L.T., Yuan, E.L., Ding, H.X., Ye, H.C., Zhang, Z.K., Yan, C., Liu, Y.Q., Feng, G., 2014. Antifungal Activity of Compounds Extracted from Cortex Pseudolaricis against Colletotrichum gloeosporioides. J. Agric. Food. Chem. 62 (21), 4905–4910.

Zhang, Z.J., Zeng, Y., Jiang, Z.Y., Shu, B.S., Sethuraman, V., Zhong, G.H., 2018. Design, synthesis, fungicidal property and QSAR studies of novel-carbolines containing urea, benzoylthiourea and benzoylurea for the control of rice sheath blight. Pest. Manage. Sci. 74 (7), 1736–1746.

Zhou, Q., Tang, X.M., Chen, S., Zhan, W.L., Hu, D., Zhou, R., Sun, N., Wu, Y.J., Xue, W., 2022. Design, Synthesis, and Antifungal Activity of Novel Chalcone Derivatives Containing a Piperazine Fragment. J. Agric. Food. Chem. 70 (4), 1023–1036.

Zou, X.M., Fu, C.R., Wang, X., Shan, P.C., Liu, J., Yang, Y.Z., Li, Y. H., Hu, F.Z., Yang, H.Z., 2017. Design, Synthesis, and Bioactivity Evaluation of Novel 3-(Substituted Phenoxy)-6-Methyl-4-(3-Trifluoromethylphenyl) Pyridazine Derivatives. J. Heterocycl. Chem. 54 (1), 670–676.

Zubrod, J.P., Bundschuh, M., Arts, G., Bruhl, C.A., Imfeld, G., Knabel, A., Payraudeau, S., Rasmussen, J.J., Rohr, J., Scharmuller, A., Smalling, K., Stehle, S., Schulz, R., Schafer, R.B., 2019. Fungicides: An Overlooked Pesticide Class?. Environ. Sci. Technol. 53 (7), 3347–3365.